Cadmium substitution in miargyrite (AgSbS$_2$) and related phases: an experimental reconnaissance

I. KELLEHER, S. A. T. REDFERN

Department of Earth Sciences, University of Cambridge, Downing Street, Cambridge, UK

AND

R. A. D. PATTRICK

Department of Earth Sciences, The University of Manchester, Manchester, M13 9PL, UK

Abstract

An experimental study of cadmium substitution into AgXS$_2$ phases (X = As, Bi, Sb) indicates significant amounts of cadmium can be incorporated in the structure by the mechanism 2Cd $\rightleftharpoons$ Ag + X. The limit of substitution of Cd in the high-temperature polymorph of miargyrite, β-AgSbS$_2$ is 6.2 at.%, whereas the low-temperature polymorph, α-AgSbS$_2$, can accommodate at least 12 at.% cadmium. Substitution of Cd into the cubic β-AgSbS$_2$ induces a small monoclinic distortion and the unit cell becomes pseudo-cubic. The α $\rightleftharpoons$ β transition in Cd-substituted miargyrites is modified by the solute ions, with both a reduction of T_c and transition smearing evident. Similar effects are also recorded in Cd-substituted AgAsS$_2$ and AgBiS$_2$.

KEYWORDS: cadmium substitution, miargyrite, As, Bi, Sb.

Introduction

AgXS$_2$ sulphosalts (in which X is As, Bi or Sb) are a group of semi-conducting sulphides that occur naturally as minor components of polymetallic sulphide ores. In addition to these relatively low-temperature, naturally occurring phases, synthetic high-temperature polymorphs exist (Table 1), forming a complex group of compounds all of which can be considered in terms of the fcc galena structure but which also display lower-symmetry derivatives. The naturally-found low temperature form of miargyrite, described here as α-AgSbS$_2$, is monoclinic but the high temperature (>380°C) polymorph, β-AgSbS$_2$, is cubic (Keighin and Honea, 1969; Graham, 1951). This high-temperature polymorph survives metastably at room temperature. Low-temperature matildite, β-AgBiS$_2$, is hexagonal (Geller and Wernick, 1959), while the high-temperature cubic form (confusingly called α-AgBiS$_2$) exists above 210°C (Hofmann, 1938; Graham, 1951). Hall (1966) synthesized three polymorphs of AgAsS$_2$; below 320°C the rhombohedral mineral trechmannite, γ-AgAsS$_2$, is stable

TABLE 1. Summary of known Ag (As,Bi,Sb)S_2 phase

Mineral name	Species/formula	Symmetry	Stability range (°C)	Reference
miargyrite	α-AgSbS$_2$	monoclinic, Cc	<380	1,2,3.4
none	β-AgSbS$_2$	cubic, fcc	>380	2,4
matildite	β-AgBiS$_2$	hexagonal	<210	1,5
schabachite	α-AgBiS$_2$	cubic	>210	1,2
trechmannite	γ-AgAsS$_2$	rhombohedral	<320 ± 5	6,7,8
smithite	β-AgAsS$_2$	monoclinic	320–415	6
none	α-AgAsS$_2$	cubic	415–421	6

References: 1, Hofmann (1938); 2, Graham (1951); 3, Knowles (1964); 4, Keighin and Honea (1969); 5, Geller and Wernick (1959); 6, Hall (1966); 7, Roland (1968); 8, Matsumoto and Norwacki (1968).

while in the temperature range 320 ± 5°C–415°C smithite, β-AgAsS$_2$, exists. A cubic form, α-AgAsS$_2$, was found to be stable between 415°C and 421°C, the latter temperature being the melting point of the mineral. In an experimental study of Cd-tetrahedrites (Pattrick and Hall, 1983), a cadmium-bearing, high temperature β-miargyrite was produced and it is the purpose of this study to examine Cd-substitution into AgXS$_2$ and related phases and its effect on the stability fields of the AgXS$_2$ structures.

Experimental methods

Samples were prepared by standard dry synthesis in evacuated silica tubes in tube furnaces at two temperatures, 361 ± 2°C and 421 ± 2°C. Starting

TABLE 2. Experimental products in the Ag-Sb–Cd–S system and Cd-concentrations in AgXS$_2$ phases

Run T (°C)	Starting Cd (at.%)	Run Products	β/α* ratio	at.% Cd in β	at.% Cd in α
AgSbS$_2$ +Cd runs					
361	0.0	α, pa	—	—	—
361	2.5	β, pa α Sb	4.7	2.9	9.4
361	5.0	β, pa, α	6.7	3.2	8.4
361	7.5	β, α, pa,	5.8	2.7	9.6
361	10.0	β, pa, α, CdS,	8.0	3.6	10.0
421	0.0	β	—	—	—
421	2.5	β, pa	—	2.9	—
421	5.0	β, CdS	—	4.8	—
421	7.5	β, CdS	—	6.0	—
421	10.0	β, CdS	—	6.2	—
AgBiS$_2$ + Cd runs					
361	7.5	α, CdS	—	3.3	—
421	7.5	α, CdS	—	—	—
AgAsS$_2$ +Cd runs					
361	7.5	α, pr, β	2.8	1.7	11.9
421	7.5	α, pr, β	12.5	—	—

(abbreviations: α = αAgXS$_2$, β = βAgXS$_2$, pa = Ag$_3$SbS$_3$, pr = Ag$_3$AsS$_3$, Sb = Sb$_2$S$_3$; the β/α ratio determined from XRD peaks).

TABLE 3. EPMA analyses of synthetic AgXS$_2$ + Cd phases (all analyses in at.%)

Run T (°C)	Starting Cd (at.%)	Ag	Sb	Cd	S
β-miargyrite					
361	2.5	24.23	23.69	2.78	49.30
361	5.0	23.90	22.96	3.96	49.19
361	7.5	24.03	22.95	4.52	48.51
361	10.0	23.58	23.31	3.63	49.49
421	0.0	26.14	25.06	0.00	48.81
421	2.5	24.84	23.88	2.65	48.64
421	5.0	23.22	22.67	5.01	49.06
421	7.5	22.71	22.45	5.92	48.92
421	10.0	22.41	22.55	6.15	48.89
α-AgSbS$_2$					
361	0.0	25.22	25.48	–	49.30
361	2.5	20.21	19.96	10.57	49.25
361	5.0	21.67	20.29	8.62	49.41
361	7.5	20.81	20.67	9.49	49.04
361	10.0	20.46	19.73	11.14	48.67
β-AgBiS$_2$					
361	7.5	23.88	24.20	3.39	48.53
β-AgAsS$_2$					
361	7.5	20.47	19.18	10.77	49.57
α-AgAsS$_2$					
421	7.5	24.17	24.29	2.35	49.19

compositions were equivalent to AgXS$_2$ with variable amounts of Cd (Table 2) and each charge was run at temperature for seven days, removed from the furnace, ground and returned to the furnace for a further seven days. Pure elements were used, except in the case of cadmium where CdS was added to starting charges. In all starting compositions the overall metal:sulphur ratio of 1:1 was maintained, such that the charges had a stoichiometry equivalent to Ag$_{1-m}$X$_{1-m}$Cd$_{2m}$S$_2$. The study focused on AgSbS$_2$ (miargyrite) phases but complementary information was produced on cadmium substitution in AgBiS$_2$ and AgAsS$_2$. Chemical analysis of the products was undertaken by electronprobe microanalysis (EPMA) using a Cameca Camebax electronprobe employing wavelength dispersive spectrometry with a take off angle of 40° and an operating voltage of 20 kV. The standards used for EPMA were α-AgBiS$_2$, CdS, ZnS, FeAsS, and CuSbS$_2$. Powder X-ray diffraction analysis of samples at room temperature was undertaken on a Philips PW 1730 X-ray generator using Cu-$K\alpha$ radiation. High-temperature differential

thermal analysis (DTA) measurements were made using a PL Thermal Sciences DTA 1500.

Experimental products

The products of the experiments were identified by optical examination, EPMA and XRD and the results are summarized in Tables 2 and 3.

AgSbS$_2$ + CdS experiments. In the high-temperature (421°C) experiments, cubic β-AgSbS$_2$ was the major constituent of the charges, the only other products being CdS and Ag$_3$SbS$_3$. EPMA (Tables 2 and 3) revealed that the β-AgSbS$_2$ contained significant amounts of cadmium. The charge with a starting composition of 2.5 at.% and 5.0 at.% Cd, produced β-AgSbS$_2$ containing ~2.9 and 4.8 at.% Cd, respectively, However, a further increase in the amount of Cd in the starting compostion did not produce a corresponding increase of Cd in β-AgSbS$_2$ and a maximum concentration (at 421°C) of 6.2 at.% Cd was attained. In the runs at 361°C, AgSbS$_2$ phases were the main products, but significant amounts of

CdS, Sb_2S_3 and Ag_3SbS_3 were also present. In the cadmium-free charges, only the low-temperature α-miargyrite formed. However, in runs in which cadmium was added, a high proportion of the high temperature β-$AgSbS_2$ was present, with α-$AgSbS_2$ a relatively minor constituent. Optical inspection and EPMA of the $AgSbS_2$ phases in the 361°C runs revealed two populations, one optically anisotropic phase containing 8–11 at.% Cd and the other isotropic 'cubic' phase with 2–4 at.% Cd (Tables 2 and 3).

AgBiS₂ + CdS experiments. At both 361°C and 421°C the high-temperature cubic α-$AgBiS_2$ polymorph was the main product, with CdS (5%) and trace amounts of other phases also present; no low-temperature, hexagonal β-maltildite was produced. The α-$AgBiS_2$ contains 3.3 at.% Cd, while grains of Ag_3BiS_3 present contain 1.1 at.% Cd.

AgAsS₂ + CdS experiments. A cubic phase, α-$AgAsS_2$, was the main product of the 421°C runs, while minor β-$AgAsS_2$ also formed, as did proustite (Ag_3AsS_3). In the runs at 361°C both the α-and β-phases are present, the latter in a significant concentration. EPMA of both the high-temperature and low-temperature runs revealed the $AgAsS_2$ phases to have two distinct cadmium concentrations, one group containing 1.0–2.4 at.% Cd, and the other 10.3–16.6 at.% Cd which coincide with the optical identification of the β- and α-phases, respectively.

In addition to optical examination, the samples were studied by back-scattered, high resolution scanning electron microscopy. This examination revealed no exsolution phenomena or evidence of fine scale intergrowths between $AgXS_2$-phases and CdS. Therefore, the solid solution of Cd in β-miargyrite is confirmed with an upper limit of 6.2 at.% Cd at 421°C, in the presence of excess CdS. Furthermore, the substitution of Cd into low-temperature α-miargyrite is higher, at least 10 at.% at 361°C. This same relationship is true of the $AgAsS_2$ phases with monoclinic β-$AgAsS_2$ accommodating higher amounts of cadmium than the high-temperature cubic α-$AgAsS_2$. The temperatures of these experiments were too high to demonstrate if this relationship is also true of matildite, but limited substitution of cadmium occurs in α-$AgBiS_2$. In all cases, the EPMA data (Table 3) demonstrate that the incorporation of the Cd is at the expense of equal amounts of Ag and Sb or Bi or As, suggesting a mechanism of coupled substitution in the form:

$$2Cd^{2+} \rightleftharpoons Ag^+ + (Sb,As,Bi)^{3+}$$
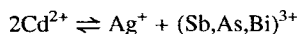
The occurrence of the cubic $AgXS_2$ phases in the 421°C runs is in agreement with existing information on these compounds. However, these experiments indicate that the incorporation of Cd greatly reduces the transition temperature to the cubic phase. The α $\rightleftharpoons$ β transition in pure miargyrite is reported as being at 380°C (Graham, 1951) but in this study the low-temperature (361°C) runs which included Cd contain more cubic miargyrite than α-miargyrite. The incorporation of Cd appears to have an even greater effect on the β-(smithite) $\rightleftharpoons$ α transition in the $AgAsS_2$ system. According to Hall (1966) this occurs at 415°C for pure $AgAsS_2$ but the Cd-bearing charges run at 361°C in this study contain cadmium-bearing cubic α-$AgAsS_2$ as the main phase.

The coexistence of both the high- and low-temperature polymorphs in the low-temperature runs clearly represents disequilibrium in these charges, presumably due to slow reaction rates and the significant metastability of the high-temperature phases below their equilibrium transition temperatures, and indicates future work will require greatly increased synthesis time if equilibrium behaviour is to be observed. To provide more information on the nature of the phase transitions in these samples, DTA was employed to examine the $AgSbS_2$–2CdS system in more detail.

X-ray diffraction analysis

The cell parameters of all the $AgXS_2$ phases were determined at room temperature and the data are presented in Table 4. The cell parameters derived for the pure high- and low-temperature $AgSbS_2$ phases were similar to those in the literature (Knowles, 1964), monoclinic symmetry is confirmed for the low-temperature α-$AgSbS_2$ phase (Table 4a) and cubic symmetry for the high-temperature pure β-$AgSbS_2$ (Table 4b). The cell parameters of the low-temperature Cd-bearing α-$AgSbS_2$ were similar to those of the pure α-$AgSbS_2$ and there is no evidence of distortion of the lattice due to Cd incorporation (Table 4a). We have refined all β-$AgSbS_2$, α-$AgBiS_2$ and α-$AgAsS_2$ assuming cubic symmetry (Table 4b) to enable comparison. The cubic, pure β-$AgSbS_2$ phase is, however, distorted by the incorporation of Cd and, furthermore, the β-$AgSbS_2$ produced in the runs at 361°C is more distorted than the β-$AgSbS_2$ produced at 421°C. The values of *a* determined from Cd-bearing β-$AgSbS_2$ at 421°C reveals a small but consistent decrease with increasing Cd content and the β-$AgSbS_2$ which contains 6.2 at.% Cd, has a unit cell size of 5.626 Å (Table 4b). This reflects the slightly smaller bond length for Cd–S of 2.52 Å compared to the average of 2.55 Å of Sb–S and Ag–S (Shannon, 1981). A slight distortion of the cubic lattice by the addition of Cd is apparent when fitting reflections such as (111), (220) and (200) to cubic symmetry, and the data are better fitted by adopting a monoclinic cell (Table 4c), indicating that the high-temperature Cd-bearing

TABLE 4. X-ray diffraction data for $AgXS_2$ + Cd phases (cell parameters in Å; standard deviations are derived from Δd_{hkl} and are *10 000, and are calculated to 4 decimal places, assuming either cubic or monoclinic (mono) symmetry)

(a) Cell parameters of α-Cd-$AgSbS_2$ phases

Run T (°C)	Starting Cd (at.%)	Cd-content α-$AgSbS_2$	a	b	c	β	Std. dev. (mono)
361	0.0	—	13.227	4.404	12.859	98.429	1
361	2.5	10.6	13.234	4.406	12.877	98.574	1
361	5.0	8.2	13.195	4.401	12.877	98.331	1
361	7.5	9.0	13.230	4.395	12.853	97.984	1
361	10.0	10.0	13.263	4.390	12.842	97.756	

(b) Cell parameters of β-$AgSbS_2$, (assuming cubic symmetry)

Run T (°C)	Starting Cd (at.%)	Cd-content β-$AgSbS_2$	a	Standard deviation
361	0.0	—	—	—
361	2.5	2.9	5.641	1
361	5.0	2.4	5.638	4
361	7.5	2.7	5.634	6
361	10.0	3.6	5.635	7
421	0.0	—	5.653	1
421	2.5	2.7	5.641	1
421	5.0	4.6	5.634	1
421	7.5	6.0	5.629	1
421	10.0	6.2	5.626	2

(c) β-Cd-$AgXS_2$ phases from Tables 4b and 4d, (assuming monoclinic symmetry)

Run T (°C)	Starting Cd (at.%)	Cd content β-$AgSbS_2$	a	b	c	β	Std. dev.
β-$AgSbS_2$							
361	2.5	2.9	5.643	5.640	5.653	90.165	0
361	5.0	2.4	5.636	5.631	5.644	90.029	1
361	7.5	2.7	5.612	5.659	5.527	88.846	1
361	10.0	3.6	5.612	5.662	5.517	88.747	1
421	0.0	—	5.654	5.654	5.649	90.000	1
421	2.5	2.7	5.643	5.638	5.650	90.111	0
421	5.0	4.6	5.633	5.634	5.631	89.937	0
421	7.5	6.0	5.628	5.630	5.630	89.940	0
421	10.0	6.2	5.629	5.628	5.623	90.103	0
α-$AgBiS_2$							
361	7.5	Cd-α-$AgAsS_2$	5.543	5.611	5.534	89.916	1
421	7.5	Cd-α-$AgAsS_2$	5.543	5.593	5.558	89.916	0

(d) Cell parameters of $AgBiS_2$ and $AgAsS_2$ phases, (assuming cubic symmetry)

Run T (°C)	Starting Cd (at.%)	phase	Cd content (at %)	a	Std. dev.
361	7.5	α-$AgBiS_2$	3.2	5.633	0
421	7.5	α-$AgBiS_2$	—	5.636	0
361	7.5	α-$AgAsS_2$	1.7	5.565	11
421	7.5	α-$AgAsS_2$	—	5.559	10

β-AgSbS$_2$ is, in fact, pseudo-cubic at room temperature. Although the value of a in β-AgSbS$_2$ synthesized at 361°C shows little variation through the suite of samples (reflecting small variations in Cd content), the fit to cubic symmetry is relatively poor and, as with the β-AgSbS$_2$ produced at 421°C, a better fit was obtained by assuming monoclinic symmetry (Table 4c). Thus, the addition of cadmium into β-AgSbS$_2$ at 361°C causes a significant distortion of the room-temperature lattice and this phase is demonstrably 'pseudo-cubic'.

Cadmium-bearing α-AgAsS$_2$ is isostructural with Cd-bearing β-AgSbS$_2$ and an even more pronounced distortion of the lattice is observed, with distinct elongation of the b axis (by almost 0.1 Å compared to a and c) and a decrease in β by 0.5° (Tables 4b,c). Similar examination of the Bragg reflections of Cd-bearing α-AgBiS$_2$, however, reveals no deviation from cubic symmetry (Table 4b) in these samples. The variation in the amount of distortion of the lattice in the various AgXS$_2$ phases reflects the decreasing difference between the covalent radius of Cd (1.48 Å) and As (1.18 Å), Sb (1.36 Å) and Bi (1.40 Å).

Phase transitions in miargyrite

Phase transitions in miargyrite and Cd-miargyrite were investigated by differential thermal analysis (DTA) over the temperature range 20°C to 420°C. Heat flow measurements were made at a heating rate of 20°C/min on a powdered sample using a PL Thermal Sciences STA 1500 instrument. Samples were heated under a constant flow of argon gas. X-ray diffraction of samples before and after each DTA run revealed no oxidation or other chemical changes. Instrument baseline measurements were made and subtracted to give reproducible sample DTA signals. The results are summarized in Table 5. The DTA traces show both endothermic and

exothermic events on heating. The specific origins of these events is best understood by first considering the least complicated DTA trace, that for cubic, pure β-AgSbS$_2$ (Fig. 1a). The first extended exothermic event corresponds to the inversion from metastable β-form to the stable low-temperature monoclinic α-polymorph. This process commences at 229°C and appears to involve two distinct exothermic events at around 242°C and 269°C. By 310°C the transformation to α-miargyrite is complete. Previous studies of the low-temperature thermal stability of β-AgSbS$_2$ (Graham, 1951) show that it remains stable at temperatures of 215°C and less, even when annealed below this temperature for long periods. Our results are in agreement with Graham's (1951) and, furthermore, show that the inversion to α-AgSbS$_2$ is a thermally activated process, only occurring at temperatures above 229°C. Above the 'metastable-β' to 'stable-α' inversion, miargyrite remains stable until approximately 367°C, at which point it transforms again to β-miargyrite as it enters the true thermodynamic stability field of the β-form. This transformation from monoclinic to cubic AgSbS$_2$ is revealed by the sharp exothermic trough which peaks at 375°C. The transition appears first-order in thermodynamic character. Although these results show that α-miargyrite is the thermodynamically stable phase below about 370°C, they also indicate the tendency of β-miargyrite to persist metastably below this temperature if quenched rapidly to room temperature from its high-temperature stability field.

Cadmium-containing miargyrites display more complex high-temperature behaviour, but in each case the DTA results can be understood in terms of the distinct polymorphic transitions occurring in each of the phases present as run products. The Cd-rich β-miargyrite containing 6.2 at.% Cd, for example, shows (on heating) the same two thermal events as seen in pure miargyrite (Fig. 1b). The presence of Cd appears to alter the limits of stability of the two

TABLE 5. Summary of the differential thermal analysis data (temperatures accurate to $\pm$5°C)

Sample description	β/α	Cd-content, at.%		Run T (°C)	β (syn)-α(DTA)*	α(syn)-β**	α (DTA)-β***
		β	α				
1 β-AgSbS$_2$	—	0.0	—	421	229	—	367
2 β-AgSbS$_2$	—	2.9	—	421	252	—	311
3 β-AgSbS$_2$	—	6.2	—	421	208	—	322
4 β and α-AgSbS$_2$	3.6	2.9	9.4	361	248	361	308
5 β and α-AgSbS$_2$	6.7	2.4	8.2	361	220	334	296

* transition temperature of quenched metastable cubic β-AgSbS$_2$ to monoclinic α-AgSbS$_2$ during heating using DTA.
** transition temperature (in samples 4 and 5) of monoclinic cadmium-rich α-AgSbS$_2$, formed during synthesis, to β-AgSbS$_2$.
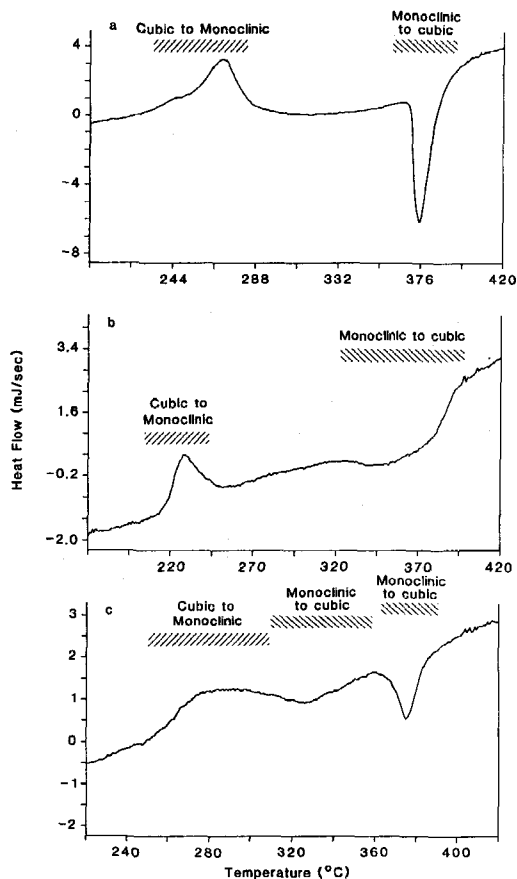*** transition temperature of α-AgSbS$_2$ formed during DTA (see *) to $\beta\beta$-AgSbS$_2$.

FIG. 1. Differential thermal analyis curves (heating) of:
a: Pure cubic β-AgSbS$_2$ synthesized at 421°C, showing
the exothermic inversion of metastable β-miargyrite to
stable monoclinic α-miargyrite at 240–270°C, followed
by the sharp $\alpha \rightarrow \beta$ endothermic trough at $\sim$375°C (see
Table 5, sample 1). b: Sample containing β-Cd-miargyr-
ite with 6.2 at.% Cd (annealed at 421°C); the influence
of Cd-defects smears out the $\alpha \rightleftarrows \beta$ transition to a broad
trough centred at around 360°C (see Table 5, sample 3).
c: A sample containing both β-Cd-miargyrite with 2.9
at.% Cd and α-Cd-miargyrite with 9.1 at.% Cd
(annealed at 361°C); at approximately 280°C the
$\beta \rightarrow \alpha$ transition results in two populations of α-miar-
gyrite being present, one low in Cd and the other high in
Cd. As a result there are two $\alpha \rightarrow \beta$ transitions, one
represented by a broad endothermic trough at
320–340°C and the other a sharp endothermic trough
at 375°C. Comparison with the data from the samples
shown in a and b, the first trough may represent the
$\alpha \rightarrow \beta$ transition of the high Cd phase, while the high-
temperature transition involves the phase containing less
Cd (see Table 5, sample 4).

phases. The breakdown of metastable β-Cd-miargyrite
to α-Cd-miargyrite occurs at lower temperatures,
between 208 and 260°C. Furthermore, the equilibrium
transition of α-Cd-miargyrite back to the high-
temperature cubic β-Cd-miargyrite is associated with
rather a broad 'smeared' exothermic trough which
begins at about 322°C, in contrast to the sharp first-
order character of the equivalent transition in Cd-free
miargyrite. The incorporation of Cd into the
miargyrite structure thus apparently causes a change
in the nature of the $\alpha \rightarrow \beta$ transition. Analogous
transition smearing has been observed at displacive
structural phase transitions in other solute-substituted
compounds (for example Cr^{3+} doped triglycine
sulphate: Strukov et al., 1980) and may be understood
in terms of the ideas developed by Levanyuk et al.
(1979). In such displacive transitions, solute ions may
be regarded as randomly distributed defects which
contribute additional excess heat capacity as the
transition is approached from below and provoke
local crystal lattice heterogeneities. Defect-defect
interactions impose effective internal lattice deforma-
tions which not only smear the transition temperature
(to a continuous distribution of local transition
temperatures) but also stabilize one phase with
respect to the other. While the reconstructive nature
of the $\alpha \rightarrow \beta$ transition in Cd-bearing miargyrite
cannot proceed in a similar manner, it is interesting to
note that Cd in this system induces a similar smearing
effect and this suggests that the potentially inhomo-
geneous Cd-distribution is modifying the reconstruc-
tive transformation on a local length scale. We
certainly observe that the $\alpha \rightarrow \beta$ transition in Cd-
miargyrite occurs at a lower temperature than that in
pure AgSbS$_2$. Other samples studied by DTA display
even more complicated signals as they contain both β-
and α-miargyrite in the starting material and the Cd-
content of each phase is different (see Fig. 1c).
Furthermore, the results suggest that the mode of
incorporation of Cd into the two phases is different.
The $\alpha \rightarrow \beta$ phase transition in material which has
undergone transformation from the metastable α-form
to the β-form at a lower temperature appears to be
different in character (as well as having a different
transition temperature) to that occurring in material
which has been crystallized in the α-stability field (see
Table 5).

Substitution mechanisms

The modes of substitution of Cd into β-miargyrite
and α-miargyrite appear to be different, as may be
expected in view of the difference in crystal structure
of the two polymorphs. While β-Cd-miargyrites do
not readily accept more than 6 at.% Cd (and then
only when there is a large excess of Cd in the total
charge), the α-Cd-miargyrites produced contained

8–12 at.% Cd at the expense of $Ag^+ + Sb^{3+}$. It seems most likely that structural changes associated with the $\alpha \rightleftharpoons \beta$ polymorphic transition account for the differences in the readiness of Cd to substitute into the two miargyrite polymorphs. We have observed that the effect of substitution of Cd into the β-miargyrite unit cell is to decrease the overall cell volume as well as impose a slight non-cubic macroscopic distortion on the room temperature metastable structure. Thus, the high-temperature β-Cd-miargyrites appear to display a slighly monoclinic 'pseudo-cubic' unit cell. Furthermore, this monoclinic distortion becomes increasingly significant with increasing Cd-content. In contrast, the substitution of Cd into the already monoclinic α-miargyrite structure does not impose such a unit cell distortion, and we have not observed a significant change in cell size. The changes in unit cell shape may offer a means to understand the effects of Cd-substitution on the polymorphic transition. These observations in themselves may, therefore, account for the variability of ease of Cd-substitution for the two forms of miargyrite. The DTA results have been interpreted in terms of the effects of local lattice distortions on the relative stability of the two phases. The macroscopic lattice distortion due to the incorporation of Cd in turn may account for the apparent difference in substitution in the two cases. Furthermore, the effect of ordering of Ag and Sb within the structure may enhance the ease of incorporation of Cd into the α-miargyrite structure because of the changes in bond length and overall cell shape associated with ordering. While the effects may be understood in their most simple terms as lattice distortions, and may be related to differences in atomic radii of the various cation species, this does not preclude the possible importance of other stabilizing phenomena. Indeed, the observed changes in unit cell parameters and local lattice strain associated with the incorporation of Cd may themselves be secondary effects coupled to some primary stabilising process, such as electronic structural effects. It may not be coincidental that the limits and optimum solubility of Cd in miargyrites correspond to particular site occupancies, and this may shed further light on the atomistic features responsible for the effects we have observed. The limit of ≈ 12 at.% substitution of Cd into α-miargyrite corresponds to 1/4 of the cations, and thus in one unit cell four Cd^{2+} ions substitute for two Ag^+ and two Sb^{3+} ions. Since the α-structure has an ordered arrangement of cations it is possible that particular sites are more crystal-chemically favourable than others. Indeed, considering the relative lengths of the bonds of Cd-S (5.52 Å in tetrahedral coordination; Shannon, 1981) to those determined by Knowles (1964) in α-miargyrite, the Ag(1) and Sb(1)

atoms in 3-fold coordination with average $M-S$ of 2.51 Å and 2.56 Å, respectively seem the most likely sites of Cd substitution. Without further structural work on these Cd-substituted α-miargyrites, precise determination of the exact mode of Cd-substitution cannot be made.

In the case of β-miargyrite, the observed maximum (6.2 at.%) substitution of Cd into the structure corresponds to approximately 1/8 of the cation sites available. It is not easy to see how this relates to the structure of β-miargyrite, which has not been fully refined. The β-miargyrite unit cell contains four cations, and the ratio of 1/8 may correspond to some ordered superlattice structure. Ordering of Cd into such a superlattice might further account for the stabilization of the β-miargyrite structure at this optimum composition. If the symmetry of the ordered structure conformed to a monoclinic (pseudo-cubic) space group, this may explain why such ordering stabilizes the structure relative to higher-Cd β-miargyrites. The addition of further Cd beyond the optimum amount would destroy the superlattice symmetry and reduce the order (and hence low-temperature stability) of such a structure.

Summary

It is clear from this study that there is significant substitution of Cd in $AgXS_2$ phases. The limit of substitution in β-$AgSbS_2$ is 6.2 at.% Cd but it is at least 12 at.% Cd in α-$AgSbS_2$. Cadmium substitution in β-$AgSbS_2$ causes distortion of the cubic lattice towards a monoclinic symmetry and it greatly reduces the $\alpha \rightleftharpoons \beta$ transition temperature. The limited amount of data on $AgAsS_2$ and $AgBiS_2$ also indicate that there is significant Cd substitution in these compounds. Further work on miargyrites should focus on Cd substitution into the low-temperature phase and the determination (perhaps by X-ray absorption spectroscopy) of the nature of substitution in both polymorphs. A similar systematic survey needs to be carried out on Cd-$AgAsS_2$ phases although Cd-$AgBiS_2$ phases appear to be less rewarding. The substitution of the other Group Vb elements, Zn and Hg into $AgXS_2$ phases might also be assessed and work could be extended to $CuXS_2$, $AgXSe_2$ and $CuXSe_2$ compounds. The whole group of $(Cu,Ag)(Sb,As,Bi)(S,Se)_2$ phases are semi-conductors with a range of electronic properties. There is decrease in light absorption (especially at the red end of the visible spectrum) in the sequence As → Sb → Bi, in part due to a reduction of the band gap. The incorporation of Cd (and perhaps Zn and Hg) into these compounds provides a large number of unexplored new compounds in which the electronic structure can be greatly varied with the potential for commercial exploitation.

References

Geller, S. and Wernick, J.H. (1959) Ternary semi-conducting compounds with sodium chloride-like structures: AgSbS$_2$, AgSbTe$_2$, AgBiS$_2$ and AgBiSe$_2$. *Acta Crystallogr.*, **12**, 46–54.

Graham, A.R. (1951) Matildite, aramayite, miargyrite. *Amer. Mineral.*, **36**, 436–49.

Hall, H.T. (1966) *The systems Ag–Sb–S, Ag–As–S and Ag–Bi–S: phase relations and their mineralogical significance.* Unpublished Ph.D. thesis, Brown University, USA.

Hofmann, W. (1938) Die struktur von miargyrit, AgSbS$_2$. *Sitz. Preuss. Akad. Wiss. Phys. Math. KL,* **VI**, 111–9.

Keighin, C.W. and Honea, R.M. (1969) The system Ag–Sb–S from 600°C to 200°C. *Mineral. Deposita,* **4**, 153–71.

Knowles, C.R. (1964) A redetermination of the structure of miargyrite, AgSbS$_2$. *Acta Crystallogr.,* **17**, 847–51.

Levanyuk, A.P., Osipov, V.V., Sigov, A.S. and Sobyanin, A.A. (1979) Change of defect structure and the resultant anomalies in the properties of materials near phase transition points. *Sov. Phys. JEPT,* **49**, 176–88.

Matsumoto, T. and Nowacki, W. (1968) The crystal structure of trechmannite, AgAsS$_2$. *Z. Krist. Min.,* **129**, 163–77.

Pattrick, R.A.D. and Hall, A.J. (1983) Silver substitution into zinc, cadmium, and iron tetrahedrites. *Mineral. Mag.,* **47**, 441–51.

Roland, G.W. (1968) Synthetic trechmannite. *Amer. Mineral.,* **53**, 1208–14.

Shannon, R.D. (1981) in *Structure and Bonding in Crystals* (M. O'Keeffe and A. Navrotsky, eds.), Academic Press, 55–70.

Strukov, B.A., Tavaskin, S.A., Minaeva, K.A. and Fedorikh, V.A. (1980) Critical phenomena in perfect and imperfect TGS crystals. *Ferroelectrics,* **25**, 399–402.